In-silico Design and Validation of Novel Lactate Dehydrogenase Inhibitors for Cancer Therapy

Anant Asthana

Abstract

Lactate is an important metabolite in both cancer and non-cancer cells. A class of enzymes known as lactate dehydrogenases, LDHs, allows cancer cells to transform excess pyruvate into lactate in anaerobic respiration, and then reconvert lactate into pyruvate for ATP production. Lactate has been shown to mediate immunosuppression and metabolic rewiring in tumors, accelerating tumor progression. Thus, developing new effective therapeutics against the action of LDH is critical to choking the Warburg effect in various types of cancer. We use the DepMap portal to identify LDH isoforms LDHA and LDHB as potential targets for cancer therapy and show that the LDHA target has a high predictive power for prognosis across many different cancers. We then use in silico techniques, such as virtual screening, pharmacophore modeling, protein structure analysis, and inhibitor selectivity analysis to design novel and effective small molecules that can inhibit both LDHA and LDHB, potentially addressing lactate-mediated immunosuppression and tumorigenesis. This study pushes forward an in-silico-centered pre-clinical ligand-based drug discovery pipeline to create optimal results in short amounts of time obviating the need for traditional expensive trial-and-error methods.

Introduction

All cells require energy to survive; for many cells, that energy comes in the form of ATP. However, the amount of ATP present in an organism's food is not near the amount of ATP that the organism as a whole requires. Thus, the cells in the organism must use a number of complex, multistep pathways to turn the proteins and sugars present in the food source, forms of stored ATP, into usable ATP.

The most common form of stored ATP is glucose, a 6-carbon aldose sugar. Cells use cellular respiration to convert glucose into ATP. Cellular respiration comes in two major forms: aerobic (if oxygen is present) and anaerobic (if oxygen is absent). The aerobic pathway is most commonly employed. Typical aerobic cellular respiration in cells uses a two-step process: first, glycolysis to turn glucose into pyruvate, and then turning pyruvate into ATP [1].

However, cancer cells require significantly more fuel and oxygen to maintain a rapid rate of proliferation. Thus, cancer cells employ anaerobic respiration: after converting glucose to pyruvate, they convert excess pyruvate into lactate. This anomaly was observed first by Warburg et al. in 1926 [2]; hence, researchers call this anomaly "the Warburg Effect." Although lactate itself can be transformed back into pyruvate for ATP production when necessary, the

presence of lactate can suppress the immune response, increase tumor resistance to therapies, enable cancer cells to communicate with nearby somatic cells, and enhance metastasis [3, 4].

Cancer cells achieve the transformation of pyruvate to lactate using a class of enzymes called lactate dehydrogenases. The production of lactate leads to concomitant oxidation of NADH to NAD+; NAD+ serves as an electron carrier that enhances the cell's ability to produce ATP [5]. Thus, developing new and effective therapeutics against the action of lactate dehydrogenases is critical to choking the Warburg effect in various cancers.

Lactate dehydrogenases (LDHs) encapsulate a family of 6 enzymes, conveniently labeled LDH1 - LDH6, each composed of one of two primary LDH subunits: LDHA, present in muscle cells, and LDHB, present in the heart. The LDHA subunit is critical for the conversion of pyruvate into lactate, and LDHB is critical for the retroconversion of lactate back into pyruvate [4]. LDHA has been more commonly observed to be upregulated in cancer cells compared to regular cells [5]. However, inhibiting only the LDHA subunit has been shown to be ineffective against cancer cells. Instead, more effective therapeutic effects are achieved when both LDHA and LDHB isoforms are inhibited [6]. Even then, metabolic rewiring within cancer cells can occur, making LDHs obsolete for the cancer's survival [7]. Thus, an effective anticancer therapy would likely involve a combination therapy of targeting LDH and other metabolic pathways, such as mTORc1 signaling-controlled metabolism [7]. In this paper, we focus on improving the state of LDH inhibition.

Pathway analysis and literature review revealed a number of LDH regulation mechanisms. Feng et al. [8] does a very thorough job of reviewing different *ldha* expression regulation mechanisms; likewise, Urbańska and Orzechowski discuss LDHB regulatory mechanisms [9]. For the sake of succinctness, we will focus on the two most notable mechanisms.

HIF1, hypoxia-inducible factor 1, is a transcription factor that is activated when the cell is in anaerobic environments. HIF1 has been shown to upregulate various key proteins in cancer progression and proliferation [10]. HIF1 binds to hypoxia-responsive elements, special 5'-RCGTG-3' DNA sequences (R is any nucleotide), in the *ldha* gene promoter region [5, 8]. HIF1 has been shown to cooperate with the MYC pathway, another regulatory pathway well-known to regulate many of the enzymes involved in glycolysis and respiration [11, 12]. c-MYC, cellular myelocytomatosis oncoprotein, is the specific protein that upregulates LDHA expression by binding to an E-box DNA sequence in the *ldha* promoter region [13].

Targeting both lactate production and LDH regulation could serve as an effective cancer treatment. Thus, it is critical to understand the regulatory pathways that upregulate LDHA, as this would allow for more informed and effective combination therapies. Notably, c-MYC is

inhibited by lactate, suggesting that starving cancer cells would involve a combination therapy targeting LDHA, HIF1, and c-MYC [5].

LDHA itself plays an important role in downstream gene regulation as well. The presence of lactate has been shown to contribute to TKI (tyrosine kinase inhibitor)-therapy resistance [14]. Acidified lactate can also be transported out of the cell and into the extracellular matrix (ECM) by MCTs, or monocarboxylate transporters [15]. Once in the ECM, lactate induces M2 polarization, which increases VEGF secretion, in turn upregulating angiogenesis [16]. Lactate has been shown to inhibit NFAT (nuclear factor of activated T cells) activity and lower IFNgamma production, which prevents proper immune response [17, 18]. Lactate also inhibits NKp64 and encourages the presence of MDSCs (myeloid-derived suppressor cells), decreasing NK (natural killer cell) cytotoxicity and immune response effectiveness towards cancer cells [3].

Thus, the overall lactate pathway produces five lactate-specific targeted cancer therapeutic strategies. Either one could target (1) the transport mechanism of lactate, (2) LDH production of lactate, (3) the transport mechanism of pyruvate into the mitochondria, (4) PDH, an enzyme that clears lactate, (5) glycolytic enzymes [19]. In this paper, we attempt to address the problem at its root by targeting lactate dehydrogenase function within cancer cells.

Target Validation

Lactate is a critical metabolite in cancer tumor progression. As mentioned above, lactate can mediate immunosuppression and angiogenesis.

In conjunction with a literature review, data analysis using the GEPIA (Gene Expression Profiling Interactive Analysis) web server was conducted to validate LDHs as targets for cancer therapeutics. As already pointed out, LDHA is overexpressed in cancer cells compared to paired control patients. Figure 1a shows *ldha* gene expression for tumor and benign samples paired by cancer type. DepMap analysis (Figure 1b) also shows how critical LDHA is for cancer cell survival across different cell lines. Most cancers rely on LDHA for their survival. Deletion of the LDHA gene from cancer cell lines had an average gene effect of -0.507 for all cancer types in the DepMap database, where gene effect < 0.5 indicates that deleting a gene is harmful to most of the cell lines. For reference, beta-actin, a protein integral to maintaining a cell's structure, has a gene effect of -0.676. Few proteins have a gene effect < -1. In addition, pan-cancer Kaplan-Meier survival curves using LDHA as the gene of interest show how patients with high LDHA either died more quickly or saw quicker tumor relapse. Thus, high LDHA is a potential biomarker of poorer aggressive cancer prognosis.
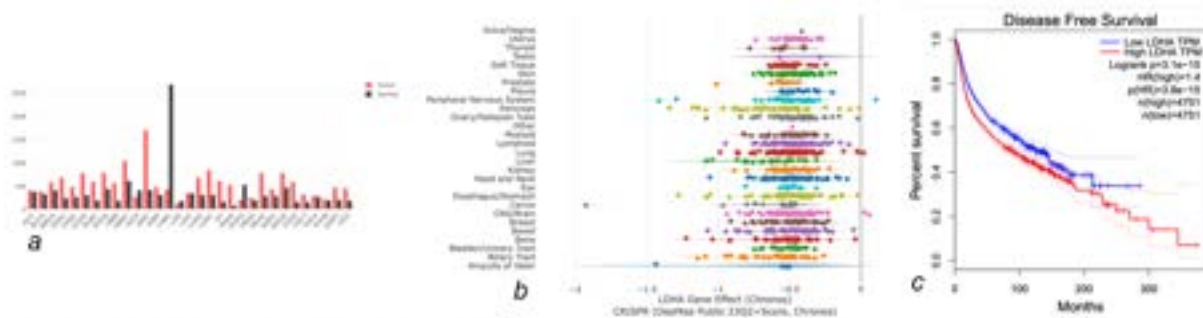
Figure 1: LDHA panel. a) For 14 out of 26 cancers, LDHA was significantly more expressed in tumor vs normal samples. Notable such cancer types are included in LUAD (lung adenocarcinoma), OV (ovarian cancer), and UCS (uterine carcinosarcoma). b) Gene effect of LDHA across cancer cell lines. Average is -0.507. c) Disease-free survival curves for LDHA. Images were adapted from GEPIA, DepMap, and GEPIA, respectively.

As shown in Figure 2, LDHB also tends to be overexpressed in some cancers, but not as frequently as LDHA. In fact, LDHB is not as critical for cell survival (as shown by a net gene effect of 0.0187, close to 0). In addition, pan-cancer Kaplan-Meier survival analysis shows that cancer progresses similarly for patients with low and high LDHB. Therefore, LDHB is not as reliable as LDHA as an indicator of cancer prognosis.
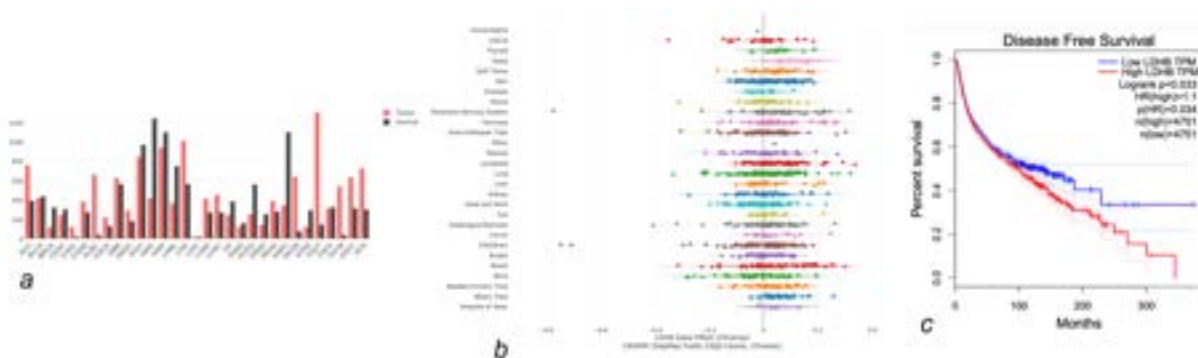
Figure 2: LDHB panel. a) For 6 out of 26 cancers (diffuse large B-cell lymphoma, skin cutaneous melanoma, tenosynovial giant cell tumor, thymoma, uterine corpus endometrial carcinoma, uterine carcinosarcoma), LDHB was significantly overexpressed in tumor vs normal samples. b) Gene effect of LDHB across cancer cell lines. Average is 0.0187. c) Disease-free survival curves for LDHB. Images were adapted from GEPIA, DepMap, and GEPIA, respectively.

Thus, it is rational to consider inhibiting LDHA selectively without attempting to target LDHB. However, inhibiting LDHA alone would produce some or no effect, whereas inhibiting both LDHA and LDHB simultaneously would lead to more potent anti-cancer effects. Even then, however, inhibiting LDHA/B leaves room for metabolic rewiring, as cancer cells turn to modifying pyruvate into bicarbonate instead of lactate [22]. Thus, an even more effective therapeutic strategy would be the inhibition of LDHA/B along with mitochondrial pyruvate transporters. Nevertheless, any combination therapy involving LDHA/B would require LDHA/B inhibitors that are potent, effective, and safe as possible. Developing such LDHA/B inhibitors is the focus of this study.

Methodology

Data Analysis and Target Validation

The Broad Institute DepMap [23-26] was used for CRISPR analysis on data from the DepMap Public 23Q2+Score and CHRONOS databases. GEPIA [24] was used for survival analysis and curve generation. GEPIA gene expression data was taken from and normalized against The Cancer Genome Atlas (TCGA) and Gene-Tissue Expression (GTEx) databases. Significant differences in gene expression between normal and tumor samples were determined by a one-way ANOVA test and p-value < 0.01.

Protein model preparation (1I10, 1I10+NADH, 7DBK, 7DBK+NADH)

It is unknown whether LDH isoforms are physiologically present in the NADH/NAD+-bound or ligand-free form. Thus, we test a molecule's average effect on both such forms. To prepare protein structures for molecular docking studies, starter structures were taken from RCSD PDB IDs 1I10 (LDH1 in complex with NADH and oxamate) and 7DBK (LDH5 in complex with NADH). 1I10 was chosen due to its good resolution (2.3 A), and 7DBK was the only human LDH1 PDB structure available. Note that the LDH1 isoform is a homomeric tetramer of LDHA subunits, while the LDH5 isoform is a homomeric tetramer of LDHB subunits.

Two protein models were created for each of LDHA and LDHB: apo- and NADH-bound, following a process outlined in [20]. The original structure with NADH was simply modified, either preserving or removing the NADH ligand, depending on the structure of interest. The structures were modified in BIOVIA Discovery Studio (free version; [33]). Note that throughout this paper, we use the terms "protein" and "receptor" interchangeably.

Virtual Screening and Result Analysis of Ligand-Receptor Interactions

Virtual screening is a technique in which large libraries of molecules are tested high-throughput using docking software or pharmacophore models. Virtual screening of small molecules against the protein structures was done using molecular docking in the PyRx software [28]. PyRx uses built-in OpenBabel for ligand preparation and AutoDock VINA for protein preparation & scoring protein-ligand complexes. Pyrx uses Monte Carlo simulation to sift through numerous different binding conformers and score each one. The default Pyrx parameters include an energy range of 3.0, exhaustiveness of 8, and mode number 9, which were used throughout the project. The scoring function takes into account entropy changes during binding; and favorable and unfavorable van der Waals interactions, hydrogen bonding, ionic forces, and aromatic

pi-pi/pi-alkyl interactions. Note that a more negative VINA score indicates a more favorable interaction.

$$VINA\ score\ =\ (\ \Delta G_0 + N_{rot}\Delta G_{rot}) + (\Delta G_{h.bond}) + (\Delta G_{ion}) + (\Delta G_{aromatic}) + (\Delta G_{lipophilic})$$

Seamdock [29 & 30] was also used for molecular docking of R-GNE-140, with parameters of energy range 3.0, exhaustiveness of 8, and mode number 9. After molecular docking, BIOVIA Discovery Studio software [31] was employed to investigate ligand-receptor interactions including pi-pi stacking, pi-alkyl interactions, conventional hydrogen bonding, and hydrophobic London dispersion interactions.

Molecular docking requires the definition of a "search space" in the shape of a rectangular box. For docking in Pyrx, the LDHA search boxes were centered near (5.5, -13.2, 152.5) and had dimensions (42.8, 55.9, 28.13), encapsulating the active site; similarly, LDHB boxes were centered near (-14.0, -9.3, 55.4) and had dimensions (44.1, 63.5, 39.8). In Seamdock, both LDHA and LDHB boxes had center (0, -17, 3) and dimensions (38, 39, 39). These parameters were kept relatively consistent by the author to minimize variation caused by experimental docking conditions.

De Novo Molecule Generation

The CReM web app [32, 33] was used to generate derivatives of GSK2837808A and R-GNE-140. The generation mode was analog (hence groups were replaced rather than scaffolded on). Molecules with synthetic accessibility <= 2.5 were considered. A context radius of 5 was used along with a fragment size of 10, and at most 150 total replacements (50 replacements, run 3 times) were considered for each of GSK2837808A and R-GNE-140 (though only 210 in total came out to be unique molecules).

Pharmacophore Modelling

A pharmacophore is a model that takes into account the important interactions between ligands and receptors and is used to computationally screen molecules at a rapid pace. Because it is not as accurate as molecular docking, it is merely used as an initial screen. Further lead optimization is carried out using molecular docking. Ligand-based pharmacophore modeling was conducted using Pharmit [34], a web server. The pharmacophores generated were based on complexes between GSK2837808A as the ligand and one of LDHA, LDHA+NADH, LDHB, or LDHB+NADH as the receptor, as well as R-GNE-140 as the ligand and one of LDHA or LDHB as the receptor. The important ligand-receptor interactions were selected based on interaction analysis in BIOVIA Discovery Studio. The library of de novo molecules has been uploaded to Pharmit and is called "round 2.1."

The fit of a ligand within a pharmacophore was calculated using the SMINA scoring function [35], which is similar to the AutoDock VINA scoring function but optimized for virtual screening. Note that SMINA may not give the same score as VINA and was only used as a preliminary score. Molecules selected based on their SMINA score were later tested to retrieve their VINA score.

ADMET and Off-Target Effects Analysis

To computationally assess ADMET properties, we employed SwissADME [36] for ADME prediction and Protox-II web server for toxicity assessment [37-39].

SwissADME uses support vector machines to test molecules against a given database of already known active molecules and predict whether a novel drug would serve as an inhibitor or substrate to a specific enzyme (notable ones including Pgp and CYP isoforms). It also uses tools such as multiple linear regressions to predict Kp (skin permeability) and Generalized Born and solvent-accessible surface area (GB/SA) to predict lipophilicity. All in all, SwissADME offers an easy–to–interpret overview of the pharmacokinetic and physiological properties of a drug. Two important methods in SwissADME include iLOGP (to calculate lipophilicity) and Ali LogS (to calculate the logarithm of solubility). The iLOGP algorithm was developed by the creators of SwissADME, and Ali LogS was created by Ali et al. [42].

Protox-II similarly uses machine learning models, such as random forest and support vector machines, and pharmacophores to predict a molecule's effect on different body systems. Protox-II's models have been trained on extensive datasets, such as the NIH LiverTox and the Carcinogenic Potency Database.

SwissTargetPrediction [43 & 44] was used to predict the targets of a given molecule, including potential off-target effects. The web server computes similarities between electroscope models of the query molecule and molecules within the server's database to compute which targets are most likely to interact most favorably with the query drug. Note that GSK2837808A was already a part of the SwissTargetPrediction database, so the algorithm predicts that GSK2837808A would target LDHA and LDHB with probability 100%. Thus, comparing this to the probabilities of de novo molecules targeting LDHA and LDHB would not be a fair comparison.

Results and Discussion

Selection of Round 1 Potency Inhibitors + Virtual Screening

Lactate dehydrogenase has been studied in the past as a possible approach to cancer treatment. However, the lactate dehydrogenase A (LDHA) subunit has been explored in much more detail than the lactate dehydrogenase B (LDHB) subunit, perhaps because LDHA is primarily found in non-heart muscle, whereas LDHB is found in heart muscle. Thus, while some FDA-approved lactate dehydrogenase inhibitors exist, none of them have been approved for cancer treatment, and all LDH inhibitors currently being developed in response to cancer are preclinical. A thorough review of the literature has offered 5 promising inhibitors of LDH that could inhibit both LDHA and LDHB in cancer cells with substantial selectivity against other dehydrogenase enzymes.

Table 1: Structures, IC50s, and binding site of 5 promising preclinical inhibitors. N.D. signifies that the IC50 was not provided in the literature. For GSK2837808A and R-GNE-140, the first value is derived from NAD(P)-Glo consumption measurements, whereas the second value is derived from NADH consumption measurements [39]. During the experiment, Galloflavin was also used for Round 1 docking, but due to its unique binding site outside of the substrate pocket, it was not considered for this project. Images are original and created using RCSD PDB structure editor.

Compound	Structure	LDHA IC50 (nm)	LDHB IC50 (nm)	Binding Mode to LDH
GSK2837808A		2.6/29.3	43/141.0	Competitive
NCI006		60	30	Competitive
NCI737		N.D.	N.D.	Competitive
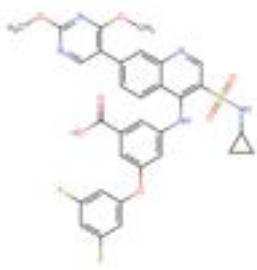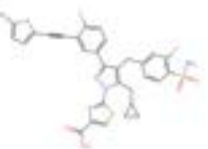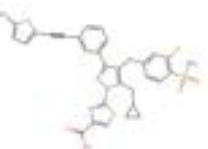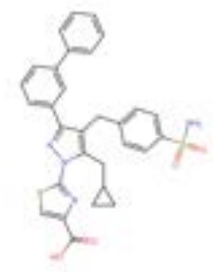
CHEMBL4081890		N.D.	N.D.	Competitive
R-GNE-140		3/6.1	5/54.3	Allosteric [41]
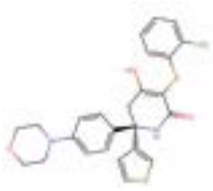
Oxamate, a common substitute for pyruvate, was used as a control to test the effectiveness of the molecular docking software. I used Pyrx to dock oxamate to LDHA+NADH and compared the results to a known crystal structure of LDHA+NADH+Oxamate (PDB:1I10).
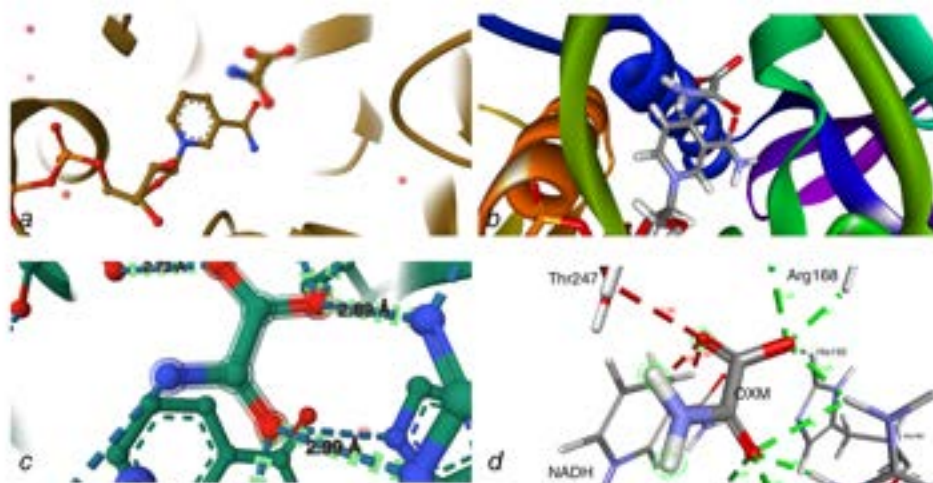
Figure 3: a & b show similar poses of oxamate in the 1I10
crystal structure and Pyrx docking output. c & d show
similar oxamate-LDHA interactions. Original images
include b and d; images a and c were adapted from the
RCSD PDB:1I10 structure.

The computational results strongly mimicked the experimental results. As shown in Figure 3, the true crystal structure of oxamate in complex with LDHA and NADH showed a very similar configuration as the molecular docking output. Thus, Pyrx docking software did a very good job of optimizing and scoring the proper conformation and orientation of inhibitors within the LDH sites. However, some notable differences were observed: firstly, docking cannot consider

important water interactions due to the constraints of software, whereas the crystal structure included NADH-water-oxamate interactions. In addition, docking did not show the crystal structure's ARG 168 NH1 - OXM O3 or Gln99 – OXM N1 interactions. Docking shows extraneous unfavorable NADH C4N – OXM O3 interaction, useful Gln99 – OXM O1 interaction, useful Arg105 NH2 – OXM O1. Docking shows an unfavorable Thr247 O1 – OXM O3 interaction, whereas crystal structure shows a useful Thr247 - OXM O3 hydrogen bond. Overall, however, Pyrx molecular docking was a viable approach for studying LDH inhibition.

As detailed in the methods section, 4 different protein structures were prepared: apo-LDHA, LDHA bound to NADH, apo-LDHB, and LDHB bound to NADH. The 5 inhibitors in Table 1 were docked to each protein structure. Interestingly, all five compounds seemed to bind more strongly to LDHB. The author is unsure why this is the case because the active sites of both LDH isoforms possess identical relevant amino acids. Another interesting note is that R-GNE-140 prefers to bind in the active site of LDHB, whereas in LDHA, it binds to the allosteric site proposed by the literature [37], as shown in Figure 4. Note that the active site of both isoforms is characterized by a loop that serves as the ceiling of the pocket. We speculate that both of these could be due to a conformational difference between LDHA and LDHB, or perhaps that because the 7DBK PDB structure is oxamate-free, it provides more space for larger molecules to fit, allowing for stronger binding affinities. Upon comparing LDHX to LDHX+NADH binding affinities, such a trend is less clearly evident.
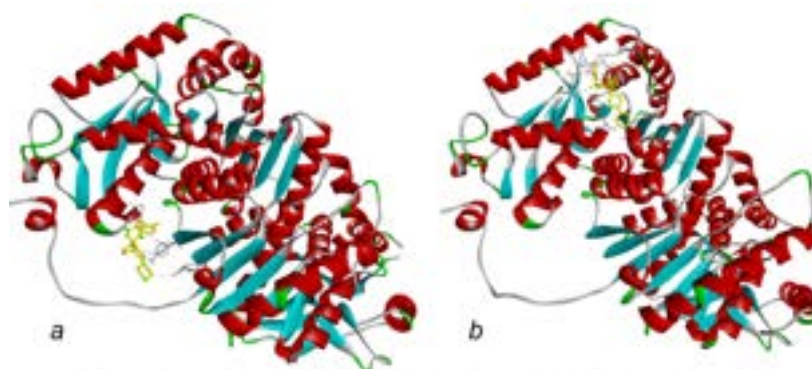
Figure 4: a shows RGNE in the allosteric binding pocket of LDHA. b shows RGNE in the active site of LDHB. Visualization done in BIOVIA Discovery Studio.

Upon examining the structures of the inhibitors in further detail, one notices that while GSK2837808A, NCI-006, NCI-737, and CHEMBL4081890 (out of which GSK2837808A bound most strongly on average to LDH) all possess relatively similar structures, R-GNE-140 does not possess a structure similar to the other four, and it potentially binds to an allosteric site on the receptor. GSK and RGNE are two promising preclinical cancer LDH inhibitors that target both LDHA and LDHB. In this paper, we identify versatile contenders that could be further optimized

to produce more selective, potent, and safe drugs than those that already exist for LDH by using GSK for active site targeting and RGNE for simultaneous allosteric and active site targeting.
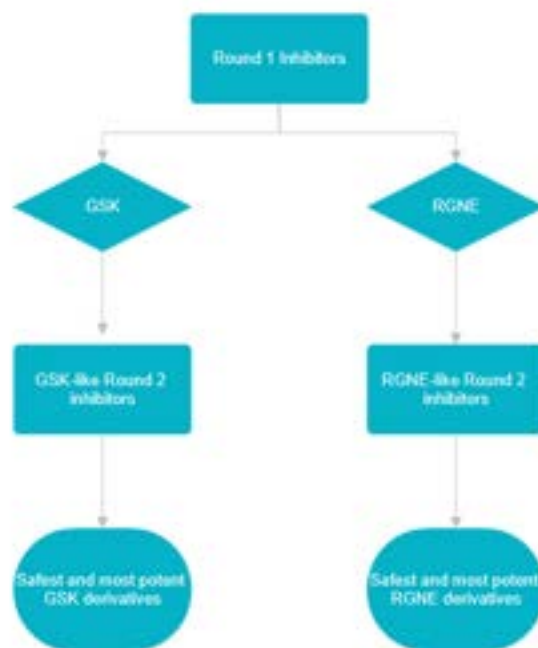
Overall experimental procedure.

Ligand-Based Pharmacophore Design and Round 2 Docking

The protein-ligand complexes of GSK with each of LDHA, LDHA+NADH, LDHB, and LDHB+NADH, as well as the RGNE complexes with LDHA and LDHB (6 complexes in total), were each used for ligand-based pharmacophore design. Simultaneously, about 210 unique de novo molecules were algorithmically generated from GSK and RGNE. These next-generation molecules were screened against all 6 pharmacophores. The molecules of interest were those that passed each pharmacophore. Here, a "pass" is defined as an RMSD (root mean square deviation) <= 2 from the original GSK/RGNE pose in the receptor (to avoid ligands that were not within the same binding pocket) and an SMINA score that was at most 0 kcal/mol (to choose only those ligands that interacted favorably with the receptor).
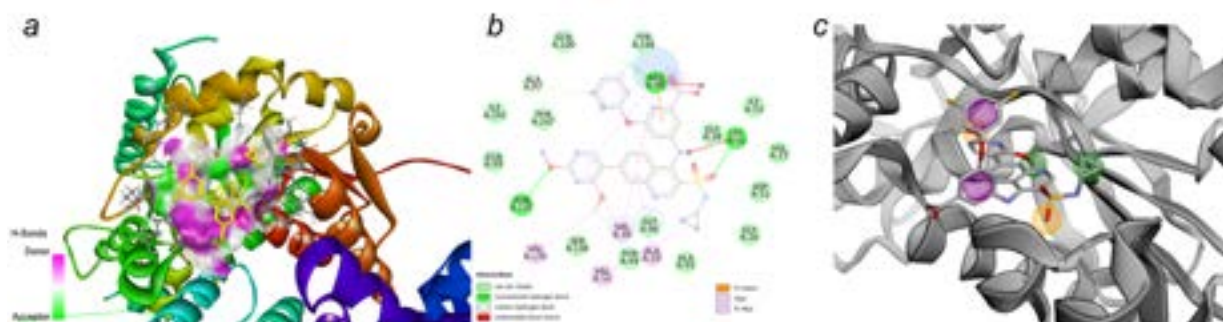
Figure 5: Example of molecular docking result (a), ligand-receptor interaction analysis (b), and pharmacophore generation (c). The light-blue surfaces around atoms in b represent solvent accessibility spheres. Images rendered in BIOVIA Discovery Studio and Pharmit.

For the GSK LDHA, LDHB, and LDHB+NADH complexes, none of the novel GSK derivatives passed the pharmacophore. However, Table 2 shows the seven molecules that passed the GSK LDHA+NADH pharmacophore that were used for further testing. In addition, ten novel derivatives passed the RGNE-LDHA pharmacophore, and two RGNE derivatives passed the RGNE-LDHB pharmacophore.

Table 2: The 7 de novo molecules that passed the GSK-LDHA+NADH pharmacophore. Images are original and created using the RCSD PDB structure editor.

Compound	Structure	SMINA Score (kcal/mol)
40		-10.1028
36		-4.86455
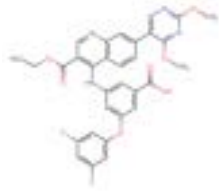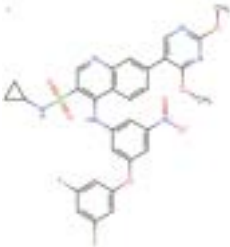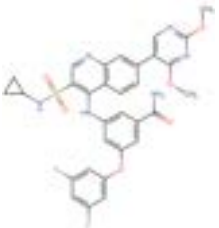
Compound	Structure	SMINA Score (kcal/mol)
7		-4.68898
41		-4.60181
6		-4.55381
45		-4.25641
39		-3.26814
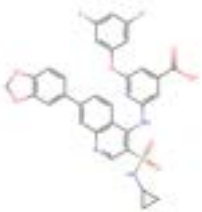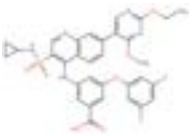
Table 3: The first ten passed the RGNE-LDHA model, and the last two passed the RGNE-LDHB model. Images are original and created using the RCSD PDB structure editor.

Compound	Structure	SMINA Score (kcal/mol)
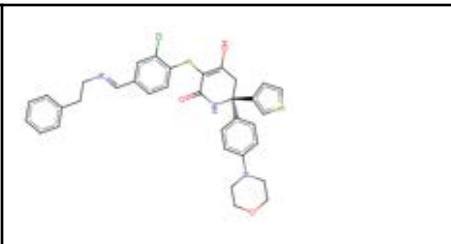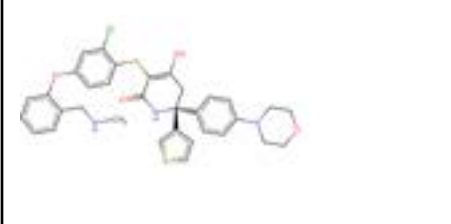
191		-7.56271
148		-6.83033
153		-6.6615
118		-6.54546
147		-6.27549
78		-6.25875
125		-6.15634
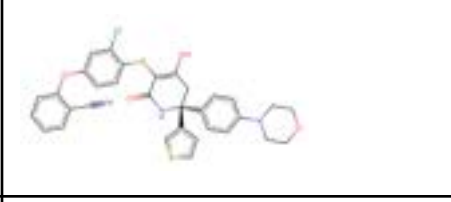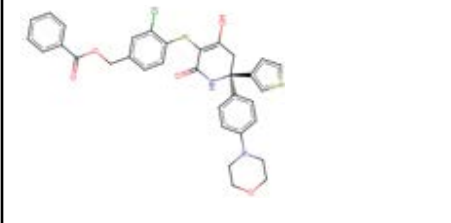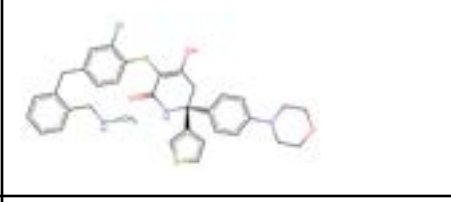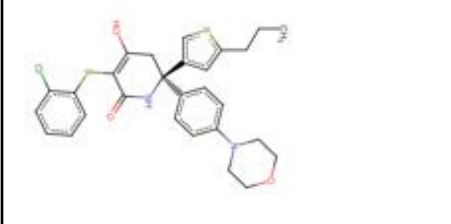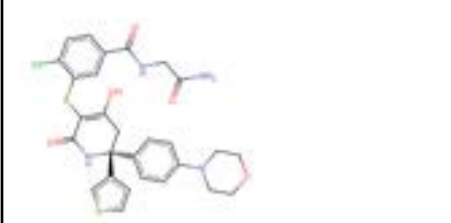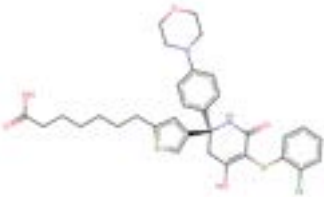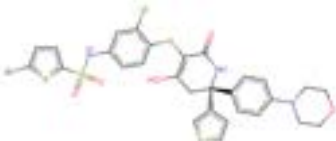
70		-5.82108
166		-5.27445
134		-4.31939
79		-9.08583
81		-7.87641
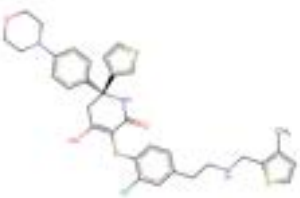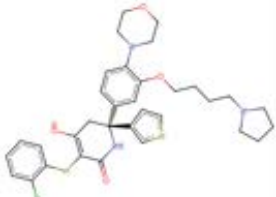
These 7 GSK derivatives and 12 RGNE derivatives underwent molecular docking to the protein structures. VINA scores for the best derivatives are shown in Tables 4 and 5.

Table 4: VINA scores for selected de novo GSK derivatives in kcal/mol. GSK is included for comparison. Of note: during molecular docking, the software automatically added a polar hydrogen atom to the nitro group of compound 41. However, this would not have affected the docking pose nor the docking score, as the algorithm considers only heavy atoms in the ligand.

Compound	LDHA	LDHA+NADH	LDHB	LDHB+NADH	Average

6	-8.8	-8.4	-10.7	-10.0	-9.5
36	-8.9	-8.9	-10.8	-10.2	-9.7
45	-9.3	-9.1	-11.5	-10.6	-10.1
GSK	-8.6	-7.4	-10.1	-10.5	-9.2

Table 5: VINA scores for selected de novo RGNE derivatives in kcal/mol. RGNE included for comparison.

Compound	LDHA	LDHB	Average
118	-9.4	-9.7	-9.6
125	-7.2	-10.3	-8.8
166	-7.6	-10.0	-8.8
191	-8.9	-9.2	-9.1
RGNE	-7.7	-9.3	-8.5

The top three GSK derivatives (compounds 6, 36, 45) four RGNE derivatives (compounds 191, 118, 125, 166) outperformed the original inhibitors and were selected for further analysis.

ADMET + Specificity Characterization

After selecting the de novo compounds that outperformed the original in potency, we investigated their ADMET properties. Tables 6 and 7 show the ADME and Toxicity results for Compounds 6, 36, 45, and GSK. SwissTargetPrediction results were used to compare the specificity of the small molecules, results shown in Table 8. Important considerations include the top few likely targets and their function.

Table 6: ADME summary for GSK and its most potent derivatives. GIA = gastrointestinal absorption. SA = synthetic accessibility. Desired properties include low iLOGP, high LogS, high GIA, fewer Lipinski violations, and low SA. None of the drugs are blood-brain barrier (BBB) permeants.

Compound	MW	Lipophilicity (iLOGP)	LogS solubility (Ali)	GIA	Lipinski violations	SA	P-gp substrate

6	648.64	3.71	-8.36	Low	2	4.41	No
36	601.56	4.32	-8.14	Low	2	4.18	No
45	631.60	4.06	-9.33	Low	1	4.26	No
GSK	649.62	3.90	-8.92	Low	2	4.41	No

Table 7: A higher tox class is safer. Active indicates potential toxicity. The toxicity properties of the GSK derivatives and GSK itself are quite similar.

Compound	Tox Class	Hepatotoxicity	Carcino-genicity	Immuno-toxicity	Muta-genicity	Cytotoxicity	Predicted LD50 (mg/kg)
6	5	Active (0.51)	Inactive (0.62)	Active (0.99)	Inactive (0.70)	Inactive (0.78)	3160
36	4	Active (0.58)	Inactive (0.69)	Active (0.99)	Inactive (0.64)	Inactive (0.68)	1000
45	5	Active (0.63)	Inactive (0.56)	Active (0.99)	Inactive (0.69)	Inactive (0.73)	3160
GSK	5	Active (0.57)	Inactive (0.62)	Active (0.99)	Inactive (0.72)	Inactive (0.77)	3160

Table 8: TargetPrediction results for GSK and its derivatives. FXa = coagulation factor X. PPAR-gamma = Peroxisome proliferator-activated receptor gamma. FLAP = 5-lipoxygenase activating protein. Aurora-B is a serine/threonine-protein kinase.

Compound	Most probable target	2nd	3rd
6	LDHA	LDHB	Thrombin/FXa
36	LDHA	LDHB	FK506-binding protein 1A
45	LDHA	LDHB	PPAR-gamma
GSK	LDHA	LDHB	Aurora-B

ADME analysis of GSK derivatives showed that compounds 6 and 36 are more soluble than GSK, making them safer to administer by mouth (though all four show low GI absorption). Compound 45 also possesses fewer Lipinski violations and is more drug-like than GSK. In addition, compounds 36 and 45 are synthetically easier to produce than GSK. Toxicity analysis shows that all four share similar toxicity hazards, but compound 36 is less safe than the others. Target prediction results show that all four have great selectivity for LDHA/LDHB. However, in terms of target selectivity, one would prefer compounds 45 and GSK over compound 6, because compound 6 targets coagulation factors. Compound 36 cannot be administered along with immunosuppressants, as it inhibits the immunosuppressant-binding protein FKBP 1A.

Overall consideration would warrant compound 45 as the most viable alternative to GSK: it is at least as safe, more drug-like, easier to synthesize, and outperforms GSK in binding affinity to the different LDH isoforms.

Similar data was collected for the RGNE derivatives.

Table 9: ADME summary for RGNE and its most potent derivatives. None of the drugs are BBB permeants.

Compound	MW	Lipophilicity (iLOGP)	LogS solubility (Ali)	GIA	Lipinski violations	SA	P-gp substrate
118	633.18	4.88	-8.92	Low	1	5.00	No
125	599.12	3.42	-6.64	Low	1	4.82	Yes
166	739.14	3.95	-10.33	Low	1	5.06	No
191	630.22	5.03	-8.82	Low	1	5.18	No
RGNE	499.04	3.86	-6.98	High	0	4.37	Yes

Table 10: Toxicity properties of the GSK derivatives and GSK itself are quite similar.

Compound	Tox Class	Hepatotoxicity	Carcino-genicity	Immuno-toxicity	Muta-genicity	Cytotoxicity	Predicted LD50 (mg/kg)
118	4	Inactive (0.55)	Inactive (0.58)	Inactive (0.73)	Inactive (0.68)	Inactive (0.64)	1000

125	4	Inactive (0.57)	Inactive (0.59)	Inactive (0.62)	Inactive (0.65)	Inactive (0.64)	805
166	4	Active (0.52)	Inactive (0.68)	Inactive (0.70)	Inactive (0.77)	Inactive (0.60)	1320
191	4	Inactive (0.60)	Inactive (0.58)	Active (0.96)	Inactive (0.69)	Inactive (0.63)	1000
RGNE	4	Inactive (0.57)	Inactive (0.58)	Inactive (0.87)	Inactive (0.71)	Inactive (0.65)	805

Table 11: TargetPrediction results for RGNE and its derivatives. Abbreviations - MELK = maternal embryonic leucine zipper. FXI = coagulation factor XI. ABL is a serine/threonine-protein kinase.

Compound	Most probable target	2nd	3rd
118	LDHA	Glucagon receptor	MELK
125	Plasma kallikrein	FXI	Glyoxalase I
166	Cannabinoid receptor 1	Cannabinoid receptor 2	ABL
191	FXI	MELK	LDHA
RGNE	Glyoxalase I	MMP-9	MMP-2

ADME analysis of RGNE derivatives showed that compound 125 had the most similar or better results than RGNE. However, while 125 is more soluble, less lipophilic, and similarly synthetically accessible as RGNE, 118 had higher predicted LD50 than 125 and RGNE, making it the safer option. In addition, both 125 and RGNE show very poor selectivity for LDH isoforms compared to 118. Target prediction studies show that 125 could have off-target effects against plasma kallikrein, which is responsible for inducing inflammation. RGNE could inadvertently inhibit glyoxalase I, responsible for detoxifying glyoxal from cells.

For these reasons, we present compound 118 as the preferred alternative to RGNE. Interestingly, 118 seems to favor LDHA's active site and LDHB's allosteric binding pocket (see Figure 5).
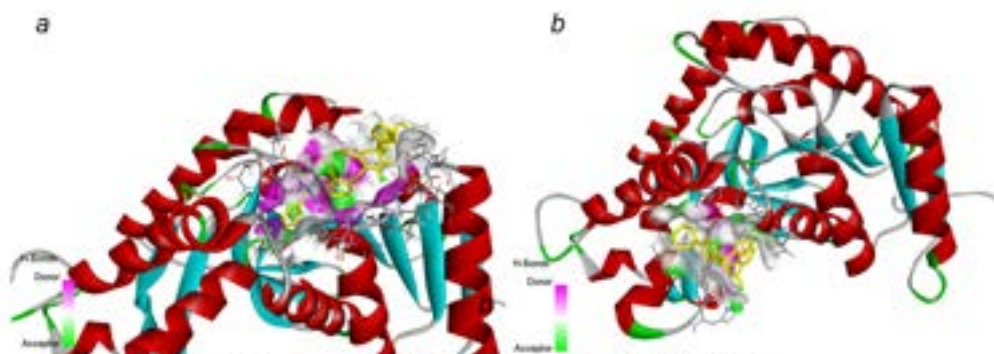
Figure 5: a shows 118 in the active site of LDHA. b shows 118 in the allosteric binding pocket of LDHB. Visualization done in BIOVIA Discovery Studio.

Conclusion

Lactate is a critical metabolite in cancer progression, and lactate dehydrogenases (LDHs) are a class of enzymes that interconvert lactate and pyruvate. LDHA, a subunit of LDH, has been observed as overexpressed across various types of cancer. Thus, inhibiting both LDHA and LDHB, the primary LDH subunits would allow for versatile cancer therapy against various conditions.

This study validated the use of molecular docking for LDH therapy design using oxamate as a control. The author used preclinical LDHA/B inhibitors (GSK2837808A and R-GNE-140) to create de novo derivatives that were well-rounded (binding well to both LDHA and LDHB, in many cases, even more so than GSK and RGNE). Finally, the ADMET and specificity properties of the new molecules were investigated to give compounds 45 and 118 as better alternatives to GSK and RGNE, where "better" is a combination of strong binding affinity and safety. Because RGNE binds to LDHA's allosteric site and LDHB's active site, 118 is versatile and could bind to either pocket. This study highlights the power of an in silico approach to drug discovery that saves time and money. All of the software used was free and open-source, as was the data collected by the researcher.

Galloflavin is another preclinical potent inhibitor of both LDHA and LDHB, though it binds to LDH just outside the binding pocket. Future research could include designing inhibitors modeled after Galloflavin, and molecular dynamics could be used to investigate how galloflavin binding affects the shape of the active site. In addition, compounds 45 and 118 could be even more thoroughly optimized for safety and then tested in vitro and in vivo.

References

1. Jerry J. Zimmerman, Amélie von Saint André-von Arnim, Jerry McLaughlin, Chapter 74 - Cellular Respiration, Editor(s): Bradley P. Fuhrman, Jerry J. Zimmerman, Pediatric Critical Care (Fourth Edition), Mosby, 2011, Pages 1058-1072, ISBN 9780323073073, https://doi.org/10.1016/B978-0-323-07307-3.10074-6.

2. Warburg O, Wind F, Negelein E. THE METABOLISM OF TUMORS IN THE BODY. J Gen Physiol. 1927 Mar 7;8(6):519-30. doi: 10.1085/jgp.8.6.519. PMID: 19872213; PMCID: PMC2140820.

3. Rabinowitz JD, Enerbäck S. Lactate: the ugly duckling of energy metabolism. Nat Metab. 2020 Jul;2(7):566-571. doi: 10.1038/s42255-020-0243-4. Epub 2020 Jul 20. PMID: 32694798; PMCID: PMC7983055.

4. Zaheed Husain, Yannu Huang, Pankaj Seth, Vikas P. Sukhatme; Tumor-Derived Lactate Modifies Antitumor Immune Response: Effect on Myeloid-Derived Suppressor Cells and NK Cells. J Immunol 1 August 2013; 191 (3): 1486–1495. https://doi.org/10.4049/jimmunol.1202702

5. Forkasiewicz, A., Dorociak, M., Stach, K. et al. The usefulness of lactate dehydrogenase measurements in current oncological practice. Cell Mol Biol Lett 25, 35 (2020). https://doi.org/10.1186/s11658-020-00228-7

6. Ždralević M, Brand A, Di Ianni L, Dettmer K, Reinders J, Singer K, Peter K, Schnell A, Bruss C, Decking SM, Koehl G, Felipe-Abrio B, Durivault J, Bayer P, Evangelista M, O'Brien T, Oefner PJ, Renner K, Pouysségur J, Kreutz M. Double genetic disruption of lactate dehydrogenases A and B is required to ablate the "Warburg effect" restricting tumor growth to oxidative metabolism. J Biol Chem. 2018 Oct 12;293(41):15947-15961. doi: 10.1074/jbc.RA118.004180. Epub 2018 Aug 29. PMID: 30158244; PMCID: PMC6187639.

7. Gaurav Pathria, David A Scott, Yongmei Feng, Joo Sang Lee, Yu Fujita, Gao Zhang, Avinash D Sahu, Eytan Ruppin, Meenhard Herlyn, Andrei L Osterman, Ze'ev A Ronai. Targeting the Warburg effect via LDHA inhibition engages ATF4 signaling for cancer cell survival. *The EMBO Journal* (2018) 37: e99735.

8. Feng Y, Xiong Y, Qiao T, Li X, Jia L, Han Y. Lactate dehydrogenase A: A key player in carcinogenesis and potential target in cancer therapy. Cancer Med. 2018 Dec;7(12):6124-6136. doi: 10.1002/cam4.1820. Epub 2018 Nov 6. PMID: 30403008; PMCID: PMC6308051.

9. Urbańska K, Orzechowski A. Unappreciated Role of LDHA and LDHB to Control Apoptosis and Autophagy in Tumor Cells. Int J Mol Sci. 2019 Apr 27;20(9):2085. doi: 10.3390/ijms20092085. PMID: 31035592; PMCID: PMC6539221.

10. Semenza, G. Targeting HIF-1 for cancer therapy. Nat Rev Cancer 3, 721–732 (2003). https://doi.org/10.1038/nrc1187

11. Semenza GL, Jiang BH, Leung SW, Passantino R, Concordet JP, Maire P, Giallongo A. Hypoxia response elements in the aldolase A, enolase 1, and lactate dehydrogenase A gene promoters contain essential binding sites for hypoxia-inducible factor 1. J Biol Chem. 1996 Dec 20;271(51):32529-37. doi: 10.1074/jbc.271.51.32529. PMID: 8955077.

12. Goetzman ES, Prochownik EV. The Role for Myc in Coordinating Glycolysis, Oxidative Phosphorylation, Glutaminolysis, and Fatty Acid Metabolism in Normal and Neoplastic Tissues. Front Endocrinol (Lausanne). 2018 Apr 12;9:129. doi: 10.3389/fendo.2018.00129. PMID: 29706933; PMCID: PMC5907532.

13. Madden, S.K., de Araujo, A.D., Gerhardt, M. et al. Taking the Myc out of cancer: toward therapeutic strategies to directly inhibit c-Myc. Mol Cancer 20, 3 (2021). https://doi.org/10.1186/s12943-020-01291-6

14. Ma R, Li X, Gong S, Ge X, Zhu T, Ge X, Weng L, Tao Q, Guo J. Dual Roles of Lactate in EGFR-TKI-Resistant Lung Cancer by Targeting GPR81 and MCT1. J Oncol. 2022 Dec 12;2022:3425841. doi: 10.1155/2022/3425841. PMID: 36545125; PMCID: PMC9763017.

15. Doherty JR, Cleveland JL. Targeting lactate metabolism for cancer therapeutics. J Clin Invest. 2013 Sep;123(9):3685-92. doi: 10.1172/JCI69741. Epub 2013 Sep 3. PMID: 23999443; PMCID: PMC3754272.

16. Pérez-Escuredo J, Van Hée VF, Sboarina M, Falces J, Payen VL, Pellerin L, Sonveaux P. Monocarboxylate transporters in the brain and in cancer. Biochim Biophys Acta. 2016 Oct;1863(10):2481-97. doi: 10.1016/j.bbamcr.2016.03.013. Epub 2016 Mar 16. PMID: 26993058; PMCID: PMC4990061.

17. Brand A, et al. LDHA-Associated Lactic Acid Production Blunts Tumor Immunosurveillance by T and NK Cells. Cell Metabolism. 2016 Nov 8;24(5):657-671. Doi: https://doi.org/10.1016/j.cmet.2016.08.011.

18. Petrella G, Ciufolini G, Vago R, Cicero DO. Urinary Metabolic Markers of Bladder Cancer: A Reflection of the Tumor or the Response of the Body? Metabolites. 2021 Oct 31;11(11):756. doi: 10.3390/metabo11110756. PMID: 34822414; PMCID: PMC8621503.

19. Pérez-Tomás R, Pérez-Guillén I. Lactate in the Tumor Microenvironment: An Essential Molecule in Cancer Progression and Treatment. Cancers (Basel). 2020 Nov 3;12(11):3244. doi: 10.3390/cancers12113244. PMID: 33153193; PMCID: PMC7693872.

20. Nilov DK, Prokhorova EA, Švedas VK. Search for Human Lactate Dehydrogenase A Inhibitors Using Structure-Based Modeling. Acta Naturae. 2015 Apr-Jun;7(2):57-63. PMID: 26085945; PMCID: PMC4463413.

21. Adams MJ, Buehner M, Chandrasekhar K, Ford GC, Hackert ML, Liljas A, Rossmann MG, Smiley IE, Allison WS, Everse J, Kaplan NO, Taylor SS. Structure-function relationships in lactate dehydrogenase. Proc Natl Acad Sci U S A. 1973 Jul;70(7):1968-72. doi: 10.1073/pnas.70.7.1968. PMID: 4146647; PMCID: PMC433644.

22. Oshima N et al., 2020, Cell Reports 30, 1798–1810 February 11, 2020 https://doi.org/10.1016/j.celrep.2020.01.039

23. DepMap, Broad (2023): This DepMap release contains data from CRISPR knockout screens from project Achilles, as well as genomic characterization data from the CCLE project. For more information, please see README.txt.. figshare. Dataset. https://doi.org/10.6084/m9.figshare.22765112.v2

24. Robin M. Meyers, Jordan G. Bryan, James M. McFarland, Barbara A. Weir, ... David E. Root, William C. Hahn, Aviad Tsherniak. Computational correction of copy number effect improves specificity of CRISPR-Cas9 essentiality screens in cancer cells. Nature Genetics 2017 October 49:1779-1784. doi:10.1038/ng.3984

25. Dempster, J. M., Boyle, I., Vazquez, F., Root, D., Boehm, J. S., Hahn, W. C., Tsherniak, A., & McFarland, J. M. (2021). Chronos: a CRISPR cell population dynamics model. BioRxiv, 432728.

26. Pacini, C., Dempster, J. M., Boyle, I., Goncalves, E., Najgebauer, H., Karakoc, E., van der Meer, D., Barthorpe, A., Lightfoot, H., Jaaks, P., McFarland, J. M., Garnett, M. J., Tsherniak, A., & Iorio, F. (2021) Integrated cross-study datasets of genetic dependencies in cancer. Nature Commmunications, 12-1661.

27. Tang Z, Li C, Kang B, Gao G, Li C, Zhang Z. GEPIA: a web server for cancer and normal gene expression profiling and interactive analyses. Nucleic Acids Res. 2017 Jul 3;45(W1):W98-W102. doi: 10.1093/nar/gkx247. PMID: 28407145; PMCID: PMC5570223.

28. Dallakyan S, Olson AJ. Small-molecule library screening by docking with PyRx. Methods Mol Biol. 2015;1263:243-50. doi: 10.1007/978-1-4939-2269-7_19. PMID: 25618350.

29. Murail S, de Vries S, Rey J, Moroy G & Tufféry P. SeamDock: An Interactive and Collaborative Online Docking Resource to Assist Small Compound Molecular Docking. Frontiers in Molecular Biosciences (2021). https://doi.org/10.3389/fmolb.2021.716466

30. Tufféry P & Murail S. Docking_py, a python library for ligand protein docking. Zenodo (2020), http://doi.org/10.5281/zenodo.4506970.

31. BIOVIA, Dassault Systèmes, Discovery Studio, San Diego: Dassault Systèmes, 2023.

32. Polishchuk, P. CReM: chemically reasonable mutations framework for structure generation. J Cheminform 12, 28 (2020). https://doi.org/10.1186/s13321-020-00431-w

33. J. Chem. Inf. Model. 2020, 60, 12, 6074–6080. Publication Date: November 9, 2020. https://doi.org/10.1021/acs.jcim.0c00792

34. Sunseri J, Koes DR. Pharmit: interactive exploration of chemical space. Nucleic Acids Res. 2016 Jul 8;44(W1):W442-8. doi: 10.1093/nar/gkw287. Epub 2016 Apr 19. PMID: 27095195; PMCID: PMC4987880.

35. Koes DR, Baumgartner MP, Camacho CJ. Lessons learned in empirical scoring with smina from the CSAR 2011 benchmarking exercise. J Chem Inf Model. 2013 Aug 26;53(8):1893-904. doi: 10.1021/ci300604z. Epub 2013 Feb 12. PMID: 23379370; PMCID: PMC3726561.

36. Daina, A., Michielin, O. & Zoete, V. SwissADME: a free web tool to evaluate pharmacokinetics, drug-likeness and medicinal chemistry friendliness of small molecules. Sci Rep 7, 42717 (2017). https://doi.org/10.1038/srep42717

37. Priyanka Banerjee, Andreas O Eckert, Anna K Schrey, Robert Preissner, ProTox-II: a webserver for the prediction of toxicity of chemicals, Nucleic Acids Research, Volume 46, Issue W1, 2 July 2018, Pages W257–W263, https://doi.org/10.1093/nar/gky318

38. Frontiers | Prediction Is a Balancing Act: Importance of Sampling Methods to Balance Sensitivity and Specificity of Predictive Models Based on Imbalanced Chemical Data Sets (frontiersin.org)

39. Malgorzata N. Drwal, Priyanka Banerjee, Mathias Dunkel, Martin R. Wettig, Robert Preissner, ProTox: a web server for the in silico prediction of rodent oral toxicity, Nucleic Acids Research, Volume 42, Issue W1, 1 July 2014, Pages W53–W58, https://doi.org/10.1093/nar/gku401

40. Vidugiriene J, Leippe D, Sobol M, Vidugiris G, Zhou W, Meisenheimer P, Gautam P, Wennerberg K, Cali JJ. Bioluminescent cell-based NAD(P)/NAD(P)H assays for rapid dinucleotide measurement and inhibitor screening. Assay Drug Dev Technol. 2014 Nov-Dec;12(9-10):514-26. doi: 10.1089/adt.2014.605. PMID: 25506801; PMCID: PMC4270152.

41. ACS Omega 2020, 5, 22, 13034–13041. Publication Date:May 27, 2020. https://doi.org/10.1021/acsomega.0c00715

42. Ali, J., Camilleri, P., Brown, M. B., Hutt, A. J. & Kirton, S. B. Revisiting the general solubility equation: in silico prediction of aqueous solubility incorporating the effect of topographical polar surface area. J. Chem. Inf. Model. 52, 420–428 (2012).

43. David Gfeller, Olivier Michielin, Vincent Zoete, Shaping the interaction landscape of bioactive molecules, Bioinformatics, Volume 29, Issue 23, December 2013, Pages 3073–3079, https://doi.org/10.1093/bioinformatics/btt540

44. Antoine Daina, Olivier Michielin, Vincent Zoete, SwissTargetPrediction: updated data and new features for efficient prediction of protein targets of small molecules, Nucleic Acids Research, Volume 47, Issue W1, 02 July 2019, Pages W357–W364, https://doi.org/10.1093/nar/gkz382